Therapeutic and imaging potential of peptide agents in cardiocascular disease

Yu, H.

6

Potent Bipartite Inhibitors of Nuclear Factor of Activated T-Cells with Superior Selectivity Compared with Cyclosporin A

Haixiang Yu*, Ilze Bot*, Xingfu Xu†, Karen Sliedregt†, Herman Overkleeft†, Gijs A. van der Marel†, Theo J.C. van Berkel*, Erik A.L. Biessen*

*Division of Biopharmaceutics, Leiden/Amsterdam Center for Drug Research, Leiden University, Leiden, the Netherlands. †Leiden Institute of Chemistry, Gorlaeus Laboratories, Leiden University, P. O. Box 9502, 2300 RA Leiden, the Netherlands

Running title:Potent bipartite peptide inhibitor of NFAT more selective than CsA

Abstract

Nuclear factor of activated T-cells (NFAT) is regarded a key target in the treatment of inflammatory and autoimmune disorders as well as cardiovascular diseases. NFAT functionality is mainly regulated by calcineurin, a multi-effector phosphatase that orchestrates T-cell activation. NFAT activation requires calcineurin docking onto NFAT and subsequent dephosphorylation. Multiple docking sites for calcineurin have recently been identified on the regulatory domain of NFAT, which may serve as template for drug design. In this study, we present a potent bipartite inhibitor of NFAT-calcineurin interaction, MCV, targeting two separate calcineurin docking sites. This inhibitor is at least equally potent as cyclosporine A (CsA) and displays sustained activity. Unlike CsA however, it is not toxic and does not impair the activity of calcineurin phosphatase, Mitogen activated protein (MAP) kinases, Bad, and NF-kB. The potency, chemical features and superior selectivity render this class of bipartite inhibitors of NFAT excellent candidates in immunosuppressant therapy as well as in cardiovascular disorders implicating NFAT activation, such as myocardiac hypertrophy, heart failure and restenosis.

Introduction

Calcineurin (CaN), a calmodulin dependent, calcium activated phosphatase, orchestrates the activation of T-, B-, NK- and mast cells as well as of all major cell types relevant to cardiovascular disease including cardiomyocytes, SMC, EC and macrophages[1]. In addition, it was shown to be a multifunctional regulator of various downstream signaling pathways. One of its downstream effectors, the family of nuclear factor of activated T-cells (NFAT C1–C4), has been implicated in osteoclast differentiation, muscle fiber-type specialization, cardiac valve development and myocardial hypertrophy[2-8]. Upon Activation calcineurin binds and dephosphorylates NFAT, which then translocates to the nucleus to induce cytokine expression. Given the important role of calcineurin-NFAT signaling in various physiological and immunological processes, its inhibition is considered as a powerful therapeutic modality in the treatment of graft transplant rejection and autoimmune diseases.

The immunosuppresants cyclosporine A (CsA) and FK506 disrupt calcineurin phosphatase activity by forming CsA-cyclophilin or FK506-FKBP12 complexes[9,10]. However, a major setback of these traditional calcineurin inhibitors is that they affect all of the downstream signal transduction pathways of calcineurin, leading to undesired side-effects and toxicity in nonimmune cells[11,12]. In search of more selective and less toxic NFAT inhibitors, much attention has been given to calcineurin-NFAT docking inhibitors that intervene in calcineurin/NFAT interaction rather than in phosphatase activity of calcineurin[13]. These efforts were given further impetus by the recent identification of a consensus motif in the N-terminal regulatory domain of NFAT, i.e. PxIxIT, as the main docking site for calcineurin[14]. Further optimization of this motif led to the discovery of MAGPHPVIVITGPHEE (VIVIT), which both as (GFP fused) peptide encoded vector (13) and as a peptide (16) selectively and potently inhibits calcineurin-NFAT interaction without impairing calcineurin phosphatase activity[15]. In addition, a series of synthetic leads, termed inhibitors of NFAT-calcineurin association (INCA), were developed which selectively interdicted calcineurin-NFAT signaling in vitro[16]. These INCA compounds unfortunately suffered from a moderate potency and cytotoxic side effect[17,18]. However, their development increased our understanding of the calcineurin configuration close to the VIVIT docking site suggesting that cysteine 266 (Cys266) within the calcineurin catalytic domain, which was deem to covalently interact with INCA, is adjacent to VIVIT binding site[19].

Despite the high selectivity of the NFAT/CaN interaction blockers as compared to CsA/ FK506 or similar calcineurin targeted immunosuppressives, the moderate potency will likely limit their clinical potential. VIVIT or INCA analogues with improved potency thus are eagerly awaited. In this study, we pursued a two-step strategy to optimize VIVIT. First the minimal essential motif of VIVIT was defined. Secondly, this motif was conjugated to an INCA analogue creating a non-toxic bipartite compound that simultaneously targets two calcineurin docking sites

and that selectively inhibits NFAT at low nanomolar potency without affecting calcineurin phosphatase activity. Given its favorable features we propose that this conjugate is an attractive lead in the development of new generation immunosuppressants.

Material and methods

Reagents

Fmoc protected amino acids, 1-hydroxybezotriazole (HOBt), 2-(1H-benzotriazole-1-yl)-1,1,3,3-tetramethyluronium tetrafluoroborate (TBTU), Fmoc-Thr(tBu)-Wang-resin were purchased from Nova Biochem (Läufelingen, Switzerland). Trifluoroacetic acid (TFA), *N*,*N*-diisopropylethylamine (Dipea), dichloromethane (DCM), dichloroethane (DCE), *N*,*N*-dimethylformamide (DMF), and piperidine were of peptide grade or higher and purchased from Biosolve (Valkenswaard, The Netherlands). FK506 was obtained from Fujisawa GmbH, Munchen, Germany; Cyclosporin A (CsA), Phorbol 12-myristate 13-acetate (PMA); ionomycin were from Sigma Chemical Company (St. Louis, MO, USA); FuGENE-6 transfection reagent was purchased from Roche Applied Science (Basel, Switzerland). Dual luciferase assay kit was from Promega (Madison, WI, USA); PDGF-BB from Biosource International Inc (Camarillo, CA, USA). 4-maleimido-benzoic acid (INCA12) was obtained from ChemBridge Europe, UK. mN-Maleimidobenzoic acid-OSu (3-MBA-OSu) was purchased from Bachem AG, Germany. Succinimidyl 4-[p-maleimidophenyl]butyrate (SMPB) was purchased from Pierce Biotechnology, USA. Bad and phosphor-Bad (Ser136) antibodies, pan-calcineurin A antibody, p44/p42 and phospho-p44/p42 MAP Kinase (Thr202/Tyr204) antibodies were from Cell Signaling Technology (Beverly, MA, USA). Rabbit anti-mouse-HRP and swine anti-rabbit-HRP antibody were from DAKO (Denmark). Anti-FLAG (M5) monoclonal and rabbit anti-actin antibodies were from Sigma (St. Louis, MO, USA). Mouse anti-HA-Tag monoclonal antibody (clone 12CA5) was from Roche Applied Science (Basel, Switzerland)

Cell culture

Murine macrophage cells (RAW 264.7), COS-1 (African green monkey kidney), human embryonic kidney (HEK293) cells and murine vascular smooth muscle cells (vSMC), isolated from thoracic aortas of male C57Bl/6 mice as described[20], were grown in Dulbecco's modified Eagles's medium (DMEM) supplemented with 10% (v/v) heat-inactivated fetal bovine serum (FBS), 100 units/ml penicillin, and 100 μg/ml streptomycin. Jurkat cells were cultured in RPMI 1640 Medium. Cultures were maintained at 37 ºC in humidified 95% air/5% CO2. Unless otherwise stated, vSMC were growth-arrested prior to the experiments by incubating in DMEM containing 0.1% FBS for 72 h.

Plasmids and constructs

NFAT reporter plasmid (pNFAT-luc) was a kind gift from Dr. De Windt, Hubrecht Laboratory, Interuniversity Cardiology Institute Netherlands; pRL-CMV was from Promega (Madison, WI, USA); pNFAT1-GFP plasmid was kind provided by Dr.

Anjana Rao, Harvard Medical School, Boston, USA); pEBG-mBad plasmid was from Cell Signaling Technology (Beverly, MA, USA). Human AKAP79 (238-380) were amplified from cDNA of HEK293 cells by PCR, employing the following primers: 5'gcggatccgaaaaacaagatgttcaaccccagcaag3' (forward hAKAP79), 5'gcgaattcaaaaaccattagcaaaaaccctacttgc3' (reverse hAKAP79).
The PCR products of AKAP79 (238-380) were cloned into *EcoRI-NotI* and *BamHI-EcoRI* digested pGEX-4T3 plasmid (Amersham). Constructs of human pGEX-NFATC2(4-385), pGEX-Cabin-1(2143-2220) and FLAG-tagged human calcineurin Aα subunit (pEF-FLAG-hCnAα 2-389) encoded a constitutive active calcineurin were kindly provided by Dr. Juan M Redondon[21].

Solid Phase Peptide Synthesis (SPPS)

Full length MAGPHPVIVITGPHEE, truncated and alanine scanned VIVIT peptides were synthesized by Fmoc solid-phase peptide synthesis on a Multisyntech Syro Multiple Peptide Synthesizer. For MCV peptides, core sequence FmocHN-His(Trt)-Pro-Val-Ile-Val-Ile-Thr(tBu)-Wang-resin was manually synthesized by standard Fmoc chemistry. The N-terminal Fmoc group was removed by 20% piperidine in DMF. After washing with 1-Methyl-2-pyrrolidinone (NMP), 3-MBA-OSu (4eq) or SMPB (4eq,) and DIPEA (8eq) was added and progression of the reaction was monitored by Kaiser's Test until a negative signal was obtained. The resin was washed with DMF, *iso*-propanol, methanol and DCM and dried. After removal of the solvent, the peptide conjugates were cleaved off from the resin with a trifluoroacetic acid, triisopropylsilane, and water mixture (95:2.5:2.5, v/v/v). Crude peptides were purified on a preparative C_{18} RP-HPLC column (Alltech) using a BIOCAD VISION automated purification system. Purified peptides were characterized by LC-MS at Leiden Institute of Chemistry, the Netherlands.

Transient transfection and dual luciferase assay

Cells were seeded in 24 well plates at a density of $5 \cdot 10^4$ cells/well and grown in DMEM supplemented with 10% (v/v) FBS, 100 units/ml penicillin and 100 µg/ml streptomycin. After 24h, cells were co-transfected with pNFAT-Luc reporter and pRL-CMV reference plasmid (encoding Renilla luciferase) with FuGene 6 transfection reagent according to the manufacturer's instructions. One day after transfection, cells were treated with and without PMA (200 nM)/ionomycin (500 nM) in the presence or absence of CsA or peptide inhibitor for 12 h, cell lysates were prepared and simultaneously assayed for firefly and renilla luciferase activity by the Dual Luciferase Assay System (Promega) and Turner Luminometer.

SMC proliferation assay

Growth-arrested vSMC were treated with 20 ng/ml PDGF-BB in the absence or presence of pretreatment of the inhibitors. Four hours later, 1 µCi/ml of [^{3}H]-thymidine was added to the vSMC and left to incubate for another 20h. Cells were washed three times with 1ml ice-cold phosphate buffered saline (PBS) and lysed in 500 µl 0.1M NaOH. Cell lysates were transferred to a liquid scintillation vial and 4.5 ml Emulsifier-Safe was added (Packard-Biosciences, Groningen, the

Netherlands), after which the radioactivity was measured in a liquid scintillation counter.

MTT [3-(4,5-dimethylthiazol-2-yl)-2,5-diphenyltetrazolium bromide] assay

RAW, vSMC and H5V cells (2,000 cells/ 200 µl medium) were seeded in 96 well plates and left to attach overnight. Cells were then treated with VIVIT, MCV1, CsA and INCA12 (0.001, 0.01, 0.1, 1 and 10 µM). After incubation for 24 hours cells were washed once with PBS and MTT (0.5 mg/ml) was added to each well. After 3 hours of incubation, the MTT solution was removed and DMSO (100 µL) was added to the cells. The cells were shaken for 30 min and absorption at 550 nm was measured on an Argus 300 Packard plate reader.

Glutathione s-transferase (GST) pull-down assay

All GST fusion proteins were expressed in Escherichia coli strain BL21 (DE3) pLys (Novagen). An overnight culture was diluted 1:100 and grown until the $A_{600\ nm}$=0.8. Production of fusion protein was induced by adding 1 mM isopropyl β-D-thiogalactopyranoside (IPTG) for 3 h at 37°C, and cell pellets were collected and suspended in lysis buffer (50 mM Tris, pH 7.5, 150 mM NaCl, 0.5 mM EDTA, 1% Triton X-100, 1x full protease inhibitor tablet (Roche), 1.5 mg/ml lysozyme, 0.02% benzonase). The soluble proteins were purified with Sepharose 4B beads (Amersham Biosciences). The purified GST protein content was confirmed by Coomassie staining on SDS-PAGE. GST fusion proteins were employed as baits in pull-down experiments. Briefly GST-containing beads were washed with lysis buffer and incubated for 30 min under gentle shaking at 4 °C with 40 µl of lysates of HEK 293 cells transfected with FLAG-tagged hCnAα constructs. Beads were then washed five times with 1 ml of lysis buffer, and bound protein was eluted by boiling samples for 5 min in the presence of 1x Laemmli buffer. Samples were loaded onto an SDS-PAGE gel and transferred to nitrocellulose membranes, after which proteins were detected by Western blotting.

Western immunoblotting

Cells were lysed in 1x Protein loading buffer and were boiled for 5 min and separated by electrophoresis by SDS-PAGE. Proteins were transferred to polyvinylidene fluoride (PVDF) membranes and then incubated in blocking solution (5% (w/v) milk/PBST (0.1% Tween 20 in PBS)) for 60 min at room temperature. To detect ERK activation, the membranes were probed with anti-phospho-p44/42 antibody (0.1% (v/v)) in 5% BSA/PBST for 1h at room temperature followed by incubation for 1h with horse radish peroxidase-conjugated secondary swine anti-rabbit antibody (0.05% (v/v)) in 5% (w/v) milk/PBST. Bad dephosphorylation was detected after 1h incubation with anti-phosphor-Bad (Ser136) antibody (0.05% (v/v)) in 5% (w/v) BSA/PBST followed by 1h incubation with rabbit swine anti-rabbit antibody (0.05% (v/v)) in 5% (w/v) milk/PBST. Total Bad and anti-actin control was used at 1:1000 dilution in 5% (w/v) BSA/PBST. To detect NFAT dephosphorylation, membranes were incubated for 1h with mouse monoclonal anti-HA antibody 12CA5 (0.05% (v/v)) in 5% (w/v) milk/PBST followed by 1h incubation with rabbit anti-mouse IgG-HRP (0.05%

(v/v)) in 5% (w/v) milk in PBST. To detect FLAG-tagged proteins, membranes were incubated for 30 min with mouse monoclonal M5 anti-FLAG antibody (0.02% (v/v)) and incubated for 30 min with rabbit anti-mouse IgG-HRP (0.05% (v/v)) in 5% (w/v) milk in PBST. After extensive wash in PBST and PBS, proteins were visualized by ECL-plus detection system according to the manufacturer's instructions (GE life sciences). Equal loading was checked by Ponceau S staining.

Immunofluorescence Analysis

COS-1 cells were cultured on coverslips and transfected with pNFAT1-GFP or YFP-p65 by FuGENE6 transfection reagent (Roche Diagnostics). Twenty four hours after transfection, cells were incubated for 1h at 37^{o}C with or without CsA or peptide inhibitor, after which cells were stimulated for 20 min with 1 μM of ionomycin and examined on a Leica fluorescent microscope. For the calcineurin-NFAT co-translocation study, COS-1 cells were cultured on cover slips and transfected with pNFAT1-GFP as described above. Twenty four hours after transfection, cells were incubated for 1h at 37^{o}C with or without MCV1 or CsA, after which cells were stimulated for 20 min with 1 μM ionomycin. Cells were then fixed with 4% formaldehyde in PBS for 15 min at room temperature, washed three times in PBS and permeabilized with 0.25% Triton X-100 in PBS for 10 min at room temperature. Permeabilized cells were incubated in blocking buffer (5% normal goat serum in PBS/0.3% Triton X-100(PBS/Triton) for 60 min, followed by 1h incubation with a 1:500 dilution of pan-calcineurin A antibody (CST) in PBS/Triton. The subcellular localizations of NFATc2 and endogenous CnA were visualized after incubation for 1h with 1:1000 diluted goat anti-rabbit IgG Alexa 555 (Molecular Probes). Cells were incubated with DAPI working solution (Molecular Probes) for 30 min at room temperature before mounting the coverslips. Nuclear localization was quantified by scoring 10 randomly selected microscopic fields containing approximately 100 cells of three different cell cultures (60X Zoom).

Modeling of MCV1 docking to calcineurin

Docking simulation was performed essentially as described previously[22]. The structure coordinates of calcineurin A (green) and calcineurin B (blue) were obtained from the 1TCO (PDB entry). The structure of the ligand, MCV1, was built using the Cambridge chemDRAW. AutoDock 3.0 was used to perform the docking. The docking space was 120 Å×100 Å × 80 Å in volume and with a grid of 3.75 Å. For the Larmarck genetic algorithm, the numbers of energy evaluations and populations were set at 10 million and 50, respectively. A total of 50 simulation runs was carried out. The number of active torsions for the ligand was 30.

Statistical Analysis

Values are expressed as mean ± SEM. A two-tailed unpaired Student's t-test was used to compare individual groups. A level of $P<0.05$ was considered significant.

Results

Identification of the domains within VIVIT essential for effective NFAT inhibition

Recent studies have revealed that VIVIT (MAGPHPVIVITGPHEE), or truncated analogues thereof such as SGPSPRIEITPSH and GPHPVIVITGPHEE, were able to inhibit NFAT activation either when fused to green fluorescent protein(GFP)[23,24] or as a peptide[25]. As conceivably not all of the amino acids within VIVIT will be equally essential for efficient blockage of calcineurin-NFAT docking, we pursued alanine scan and truncation studies to pinpoint the minimal essential core motif of VIVIT. First we have stepwisely truncated VIVIT at the N-, C- and N+C-terminus and tested NFAT inhibitory activity of the peptides in a cellular reporter assay in RAW cells. The VIVIT parent peptide was used as a reference (Fig. 1A). Deletions at the N- and the C-terminal end of VIVIT were found to be tolerated as long as the PxIxIT motif within VIVIT was preserved. Subsequent alanine scan studies confirmed the critical importance of the HPVIVI core motif (Fig. 1B). Gly(3) seems to be a preferred amino acid at this position, while the val (9) could be replaced by alanine without loss in potency and mutation of Thr(11) only moderately impaired the inhibitory activity of VIVIT. Summarizing, we demonstrate that not all the amino acids of VIVIT are required for NFAT inhibition and identify (Gx)HPVIVI(T) as core motif for subsequent optimization studies.

Based on these findings we have in the second step, synthesized four core peptides: HPVIVI, HPVIVIT, GPHPVVI and GPHPVIVIT. While these peptides appeared to be equally potent in the macrophage based NFAT reporter assay, they differed in their ability to ablate platelet-derived growth factor-BB (PDGF-BB) mediated vascular smooth muscle cells (vSMC) proliferation (Fig. 1C). HPVIVIT and GPHPVIVIT were much more potent in this assay than HPVIVI or GPHPVIVI, indicating that the threonine in the PxIxIT motif is strictly required. Interestingly, HPVIVIT displayed even stronger inhibition than the parent peptide and was almost 10-fold more potent than GPHPVIVIT (Fig. 1C). Therefore, we chose HPVIVIT as the shortest motif of VIVIT.

Maleimide conjugated VIVIT peptides exhibit low nanomolar potency for NFAT inhibition

In the next step we have optimized the core motif, taking advantage of the recent finding that INCA compounds inhibit NFAT/calcineurin interaction by binding to Cys266 at close distance (>15 Å) of the putative VIVIT binding cleft[26]. Therefore, we have conjugated two phenyl maleimide groups to the N-terminal amino group of HPVIVIT, in order to generate a bipartite antagonist of NFAT, that binds simultaneously to the VIVIT and to the maleimide binding cleft (Fig. 2A). To stretch the 15 Å gap between the two sites we conjugated the maleimide to HPVIVIT via a linker arm ranging from 8-27.6 Å, which is well beyond the estimated distance between the Cys266 and the VIVIT binding groove on calcineurin. Two of maleimido conjugated VIVIT peptides, MCV1 and MCV2

were able to inhibit NFAT activation to basal levels at 100 nM, whereas HPVIVIT or INCA12 were completely ineffective at this concentration. Also MCV3 and MCV4 appeared to be more potent than HPVIVIT. The latter two however were unable to totally prevent ionomycine/PMA stimulated NFAT activation (Fig. 2B). The IC50 values of MCV1 and MCV2 are 1.9 nM and 9.9 nM respectively (Fig.2C), which is 10,000 fold more potent than the parent peptide VIVIT (IC50=30 μM). In fact, MCV1 is at least equally potent as CsA.

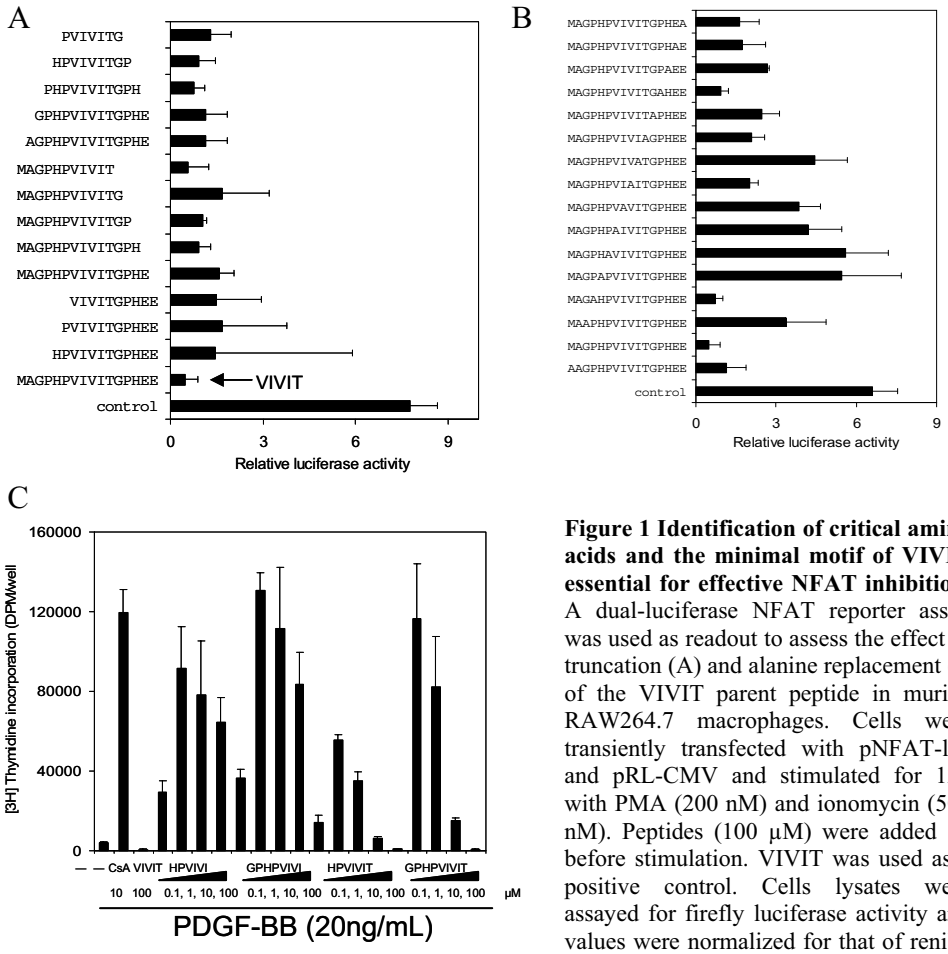

Figure 1 Identification of critical amino acids and the minimal motif of VIVIT essential for effective NFAT inhibition. A dual-luciferase NFAT reporter assay was used as readout to assess the effect of truncation (A) and alanine replacement (B) of the VIVIT parent peptide in murine RAW264.7 macrophages. Cells were transiently transfected with pNFAT-luc and pRL-CMV and stimulated for 12h with PMA (200 nM) and ionomycin (500 nM). Peptides (100 μM) were added 1h before stimulation. VIVIT was used as a positive control. Cells lysates were assayed for firefly luciferase activity and values were normalized for that of renilla luciferase. Values represent means±SD of three independent experiments. (C) To pinpoint the essential motif of VIVIT, growth-arrested vSMCs were treated for 4h with or without PDGF-BB (20 ng/mL) in the presence or absence of peptides at the indicated concentrations. CsA (10 μM) and VIVIT parent peptide (100 μM) were added as references. [^{3}H] thymidine (1 μCi/mL) was added and DNA incorporation was measured after 20h. Values represent means ±SD of three individual experiments. (** P< 0.01 versus PDGF-BB treated group).

A

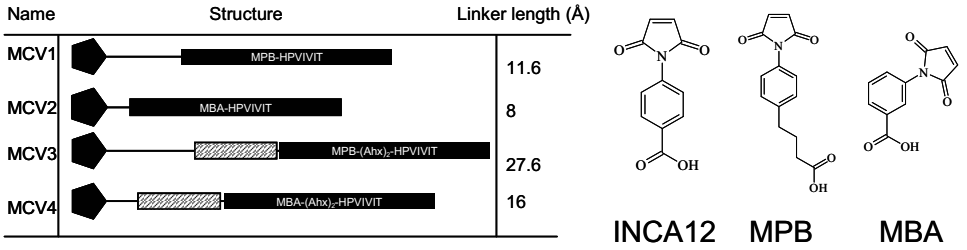
Name
Structure
Linker length (Å)
MCV1
MPB-HPVIVIT
11.6
MCV2
MBA-HPVIVIT
8
MCV3
MPB-(Ahx)2-HPVIVIT
27.6
MCV4
MBA-(Ahx)2-HPVIVIT
16
INCA12
MPB
MBA

B

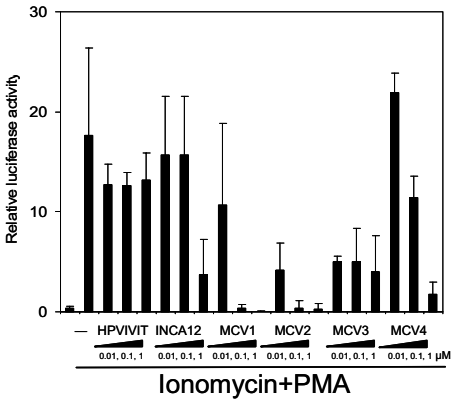
Relative luciferase activity
30
20
10
0
— HPVIVIT INCA12 MCV1 MCV2 MCV3 MCV4
0.01, 0.1, 1
0.01, 0.1, 1 µM
Ionomycin+PMA

C

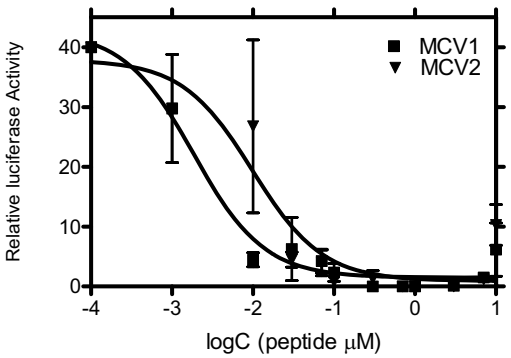
Relative luciferase Activity
40
30
20
10
0
MCV1
MCV2
-4
-3
-2
-1
0
1
logC (peptide µM)

D

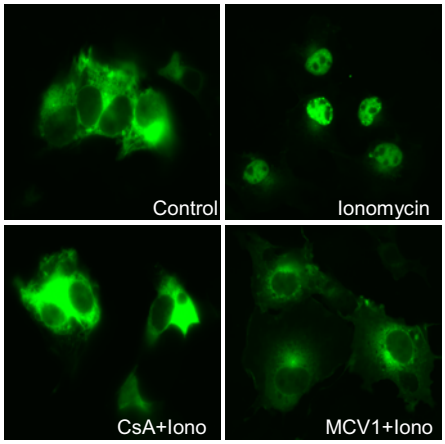
Control
Ionomycin
CsA+Iono
MCV1+Iono

E

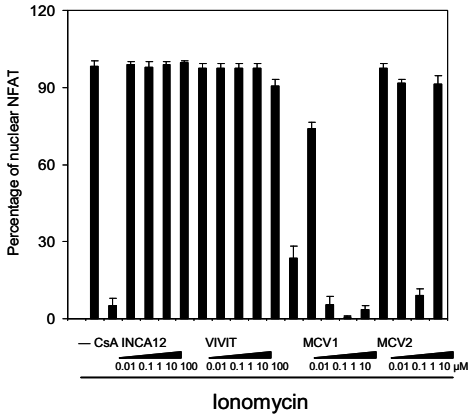
Percentage of nuclear NFAT
120
90
60
30
0
— CsA INCA12 VIVIT MCV1 MCV2
0.01 0.1 1 10 100
0.01 0.1 1 10 100
0.01 0.1 1 10
0.01 0.1 1 10 µM
Ionomycin

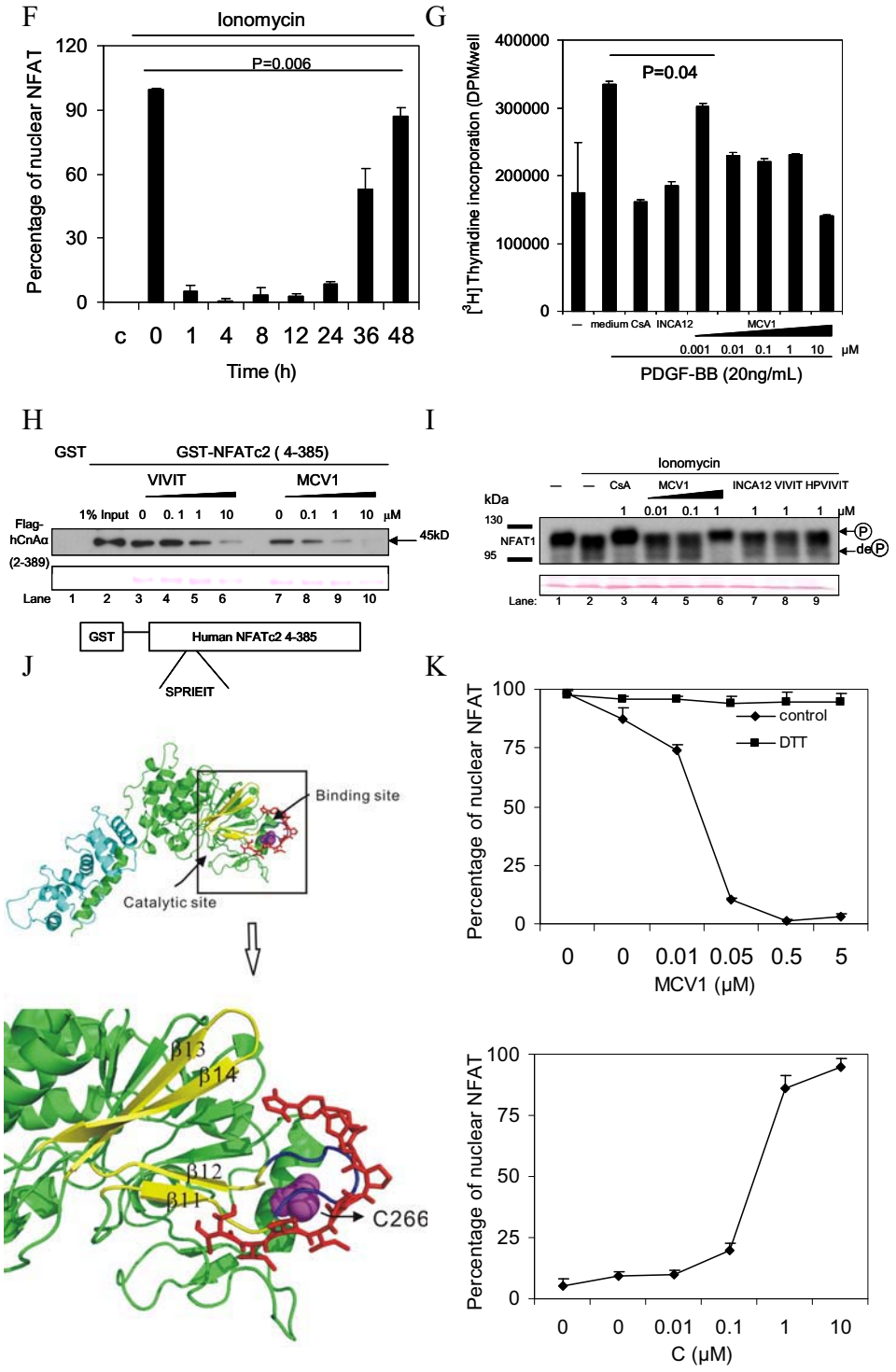
F
Ionomycin
P=0.006
Percentage of nuclear NFAT
120
90
60
30
0
c 0 1 4 8 12 24 36 48
Time (h)
G
P=0.04
[3H] Thymidine incorporation (DPM/well
400000
300000
200000
100000
0
— medium CsA INCA12 MCV1
0.001 0.01 0.1 1 10 μM
PDGF-BB (20ng/mL)
H
GST
GST-NFATc2 (4-385)
VIVIT
MCV1
1% Input 0 0. 1 1 10 0 0.1 1 10 μM
Flag-
hCnAα
(2-389)
45kD
Lane 1 2 3 4 5 6 7 8 9 10
GST
Human NFATc2 4-385
SPRIEIT
I
Ionomycin
— — CsA MCV1 INCA12 VIVIT HPVIVIT
kDa
1 0.01 0.1 1 1 1 1 μM
130
NFAT1
95
P
deP
Lane: 1 2 3 4 5 6 7 8 9
J
Binding site
Catalytic site
β13
β14
β12
β11
C266
K
Percentage of nuclear NFAT
100
75
50
25
0
control
DTT
0 0 0.01 0.05 0.5 5
MCV1 (μM)
Percentage of nuclear NFAT
100
75
50
25
0
0 0 0.01 0.1 1 10
C (μM)

Figure 2 MCV displays a dramatically enhanced potency as compared with VIVIT in NFAT inhibition. (A) Chemical structure of INCA12, MPB and MBA, as well as a schematic cartoon illustrating the MCV structures (black pentagon: maleimide; hatched box: two tandem aminohexanoic (Ahx) linker; black box: HPVIVIT peptide bone). The estimated maximal reach of the N-terminal maleimide group relative to the histidine of HPVIVIT peptide is given for each of the MCV leads. (B) A dual-luciferase NFAT reporter assay was used as readout to compare the inhibitory activities of the MCV peptides with HPVIVIT or INCA12 at indicated concentration. (C) Inhibition curves of NFAT by MCV1 and MCV2 as determined by the dual luciferase assay. (D) COS-1 cells were transfected with pNFAT1-GFP and 24h later stimulated for 20 min with ionomycin (1 μM) in the presence or absence of CsA (1 μM**)** or MCV1 (1 μM**).** Representative microscopic views illustrating that ionomycin elicited nuclear translocation of NFAT1-GFP is prevented by CsA or MCV1. (E) Quantification of the relative degree of nuclear localization of NFAT1-GFP in the absence or presence of CsA, INCA12, MCV1 or MCV2 at the indicated concentrations (in each well randomly selected microscopic fields were scored containing ±100 GFP^+ cells; values are means of three wells; **, P<0.01 versus ionomycin stimulated control). (F) NFAT1-GFP transfected COS-1 cells were incubated with 1 μM MCV1 for the indicated time. Cells were then stimulated with ionomycin (1 μM) for 20 min and nuclear translocation of NFAT1-GFP was examined. (G) Growth-arrested vSMCs were treated for 4h with or without PDGF-BB (20 ng/mL) in the presence or absence of peptides at the indicated concentrations. CsA (10 μM) and INCA12 (10 μM) were added as a control. [^{3}H] thymidine (1 μCi/mL) was added and DNA incorporation was measured after 20h. Values represent means ±SD of three individual experiments (** P< 0.01 versus PDGF-BB treated group). (H) Lysate from HEK-293 cells expressing FLAG-tagged CnA proteins were analyzed by affinity binding to GST (lane 1) and GST-NFATc2 (residues 4-385) in the presence of VIVIT (lane 3-6) or MCV1 (lane 7-10) at the indicated concentrations. Bound CnA protein was evaluated by Western blotting against FLAG tag. Ponceau S staining is provided below to illustrate equal loading of the samples. (I) pHA-NFAT1-GFP transfected COS-1 cells were stimulated for 15 min with ionomycin (1 μM) in the presence of CsA, MCV1, INCA12, VIVIT or HPVIVIT at the indicated concentrations. Multiple bands of phosphorylated and faster migrating dephosphorylated NFAT1 protein oin the cell lysates were visualized by Western blotting and anti–HA staining. Below panel depicts Ponceau staining to illustrate equal protein loading of the lanes. (J) A structure model of MCV peptide interaction with calcineurin Aα Upper panel: three dimensional structure of calcineurin-A indicating the respective positions of the catalytic and the putative peptide binding site; Calcineurin A and B are shown in green and light blue, respectively. Lower panel: high power view of the MCV1 binding site. Calcineurin A is depicted by ribbon representation, MCV1 is depicted by stick representation (red) and the loop between β11 and β12 is shown in dark blue. Cysteine 266 on the α10 helix of CnA, which is proposed to engage in a covalent interaction with maleimide group from INCA, is in magenta spheres. (K) Inhibition studies of NFAT1-GFP nuclear translocation in ionomycin (1 μM) stimulated COS-1 cells by MCV1 after preincubation of this compound for 2h at room temperature with an equimolar amount of dithiothreitol (DDT, circle) or without additive (square) (left panel) or after preincubation of the COS-1 cells with sulfhydryl reactive agent IAM (right panel). After 20 min stimulation by ionomycin cellular localization of NFAT1 was detected and quantified as compared with MCV1 pretreatment alone as a control.

Next we have explored the activity pattern of MCV1 and MCV2 peptides as compared to that of CsA. MCV1 was seen to abrogate nuclear translocation of NFAT1-GFP after ionomycin stimulation at 100 nM, whereas VIVIT showed only very little inhibition at a 100 fold higher concentration (Fig. 2D, 2E.). MCV1 thus appears to be approximately 1,000 fold more potent than VIVIT in inhibiting NFAT translocation. Remarkably, MCV2 showed potent inhibition of NFAT nuclear import at 1 μM, but lost its inhibitory capacity at 10 μM. The mechanism underlying its biphasic activity is still unclear. The most promising lead in our

study, MCV1, was characterized in more detail in subsequent experiments. The inhibitory effect of MCV1 was quite persistent (Fig. 2F). Preincubation of COS-1 cells transiently expressing NFAT1-GFP with MCV1 (1 μM) for 24h prior to ionomycin stimulation prevented NFAT translocation. Even 48h after MCV1 incubation, we did not observe a full recovery of the stimulatory effect of ionomycin on NFAT activity (10% residual cytosolic NFAT activity; P=0.006). Therefore, the half-life of MCV1 activity was estimated to be approximately 36h.
In a next set of experiments we compared the inhibitory effect of MCV1 on vSMC proliferation in vitro with that of CsA and INCA12. MCV1 (10 nM) profoundly inhibited PDGF-BB stimulated vSMC proliferation (P=0.04; -80%), while at 10 μM, it was similar effective as CsA in reducing vSMC proliferation to basal levels. (Fig. 2G).
We then tested the ability of MCV1 to compete *in vitro* with purified GST-NFATc2 (4-385) for binding to calcineurin in a pull down assay detecting GST-NFAT bound calcineurin by anti-FLAG directed immunoblotting (Fig. 2H). Also here MCV1 was already effective at 100 nM while completely disrupting calcineurin-NFAT interaction at 10 μM, whereas conversely VIVIT showed weaker inhibitory effect at 10 μM than MCV1. Altogether MCV1 is much more potent than the parent peptide VIVIT in dissociating calcineurin-NFAT interactions.
Next we addressed whether MCV1 prevented NFAT translocation by blocking its dephosphorylation (Fig. 2I). Hereto, HA-NFAT1 transfected COS-1 cells were preincubated with MCV1, VIVIT, CsA, HPVIVIT and INCA12. After stimulation of the cells with 1 μM ionomycin, the phosphorylation status of NFAT protein in the cell lysate was evaluated by immunobloting with anti-HA antibody. Clearly, multiple proteins with a slightly higher electrophoretic mobility than phospho-NFAT became visible upon ionomycin stimulation, reflecting dephospho-NFAT. MCV1 completely inhibited the NFAT dephosphorylation at 1 μM, whereas INCA12, VIVIT parent peptide and HPVIVIT did not have any inhibitory effect at this concentration.
Molecular modeling studies of MCV1 interaction with calcineurin protein were performed to provide a mechanistic basis for the profound gain in affinity of MCV1 versus the separate building blocks HPVIVIT and INCA12. The most favorable configuration with the lowest energy is shown in figure 2J. It clearly shows that MCV1 has a distinct binding site from the catalytic site of calcineurin. Therefore, it should not impair the calcineurin phosphatase activity. The hydrophobic side chains of MCV1 are in close contact with the β11 loop, while the maleimido group is accommodated in the groove formed by the β11- β12 and β13-β14 turns. No solutions in the 20 runs with low energies were found to support the proposal that the maleimido group was in direct contact with Cys266 which was actually partially protected by β11- β12 loop. The minimal binding energy of MCV1 is -12.59 kcal/mol, which is comparable to that reported for PVIVIT (-13 kcal/mol)[27].

NFAT nuclear translocation assay in COS-1 cells in vitro was used to assess the hypothesis that there is a covalent reaction between maleimido group of MCV1 and sulfhydryl group. This option was tested by comparing the NFAT translocation inhibitory capacity of MCV-1 in transfected COS-1 cells to that of MCV-1 that had been preincubated with DTT. Pretreatment with DTT totally blunted the inhibitory effect of MCV-1 (Fig. 2K left). Likewise preincubation of the transfected COS-1 cells with sulfhydryl modifying reagents 2-iodoacetamide (IAM) dose dependently prevented the MCV-1 induced inhibition of NFAT translocation, which is in support of the occurrence of a covalent interaction between the maleimide and calcineurin derived cysteines (Fig. 2K right).

MCV leads are more selective for NFAT and less toxic than CsA

In addition to NFAT family members, calcineurin also binds endogenous regulators such as A-kinase anchoring protein 79 (AKAP79) and calcineurin binding protein-1/calcineurin inhibitor (Cabin-1/Cain). AKAP79 and Cabin-1 carry motifs with similarities to the PxIxIT consensus motif of NFAT[28,29]. Since MCV1 dose dependently disrupts calcineurin-NFAT interaction by interacting with the PxIxIT motif, conceivably it may also intervene in AKAP79 or Cabin-1 binding to calcineurin. As shown by pull down assay (Fig. 3A), binding of calcineurin to either AKAP79 or Cabin-1 was not affected by MCV1 at concentrations that suffice for effective disruption of calcineurin-NFAT interaction.

Next we turned our attention to effects on downstream effectors of calcineurin other than NFAT. Previously it was shown that calcium influx induced apoptosis proceeds through calcineurin mediated dephosphorylation of Bad[30]. Since Bad protein contains no PxIxIT motif, its dephosphorylation thus should occur in an NFAT-independent manner. We therefore investigated whether this process is influenced by MCV1 and CsA. As shown in Fig. 3B, ionomycin stimulation induced Bad dephosphorylation at Ser 136. Bad expression remained unaltered after ionomycin treatment in the presence of CsA or MCV1. Although interfering with calcineurin phosphatase activity, CsA did not inhibit ionomycin induced Bad dephosphorylation in our study, which is in keeping with previous studies[31], Interestingly, MCV1 did show some inhibition of Bad dephosphorylation at lower concentrations. This suggests that selective NFAT inhibition under conditions of Ca^{2+} influx may act anti-apoptotic, whereas calcineurin inhibition per se is inert.

NF-κB is another downstream effector of calcineurin whose activation was impaired by CsA. To demonstrate the selectivity of MCV1 in comparison with CsA, we examined YFP-p65 protein translocation after MCV1 treatment (Fig. 3C). Ionomycin induced almost quantitatively (~85%) nuclear accumulation of YFP-p65. CsA totally disrupted p65 activation and prevented its nuclear import to basal levels, whereas MCV1 showed no significant effect.

Sustained Ca^{2+} signaling and cotranslocation of calcineurin and NF-AT into the nucleus will transduce the persistent activation of NFAT mediated gene expression[32,33]. Upon ionomycin stimulation, we observed a partial (~20%) but not

complete nuclear import of the calcineurin ensuring a sufficient and sustained activation of NFAT which was not seen in unstimulated cells, whereas activated NFAT still resides within the nucleus (Fig. 3D). CsA (1 µM) completely blocked both of the calcineurin and NFAT cellular translocation. Likewise, MCV1 showed a impaired nuclear import of NFAT (Fig. 2D) but showed only little effect to that of calcineurin. Therefore, the nucleus import of calcineurin may not be necessarily associated with NFAT1 as a complex by the PxIxIT motif but in a self-governed way.

Finally, we have tested the general toxicity of intracellular signaling over MAP kinase (ERK) activation. Growth-arrested vSMC pretreated with MCV1 or CsA was analyzed by Western blotting for extracellular signal-regulated kinase (ERK) activation (Fig. 3E). Pretreatment with either MCV1 or CsA did not alter PMA induced ERK activation. Pretreatment with MCV1 alone has no effect on endogenous ERK activity as well. In contrast, although ineffective on PMA stimulated ERK activity, CsA markedly increased phosphorylated ERK levels in non-stimulated cells at concentrations as low as 0.1 µM. MCV1, unlike CsA, did not show any signs of overt cytotoxicity in macrophage RAW 264.7 as judged from an MTT assay at concentrations of up to 10 µM (Fig. 3F). A similar pattern was found in vSMC and murine endothelial cells H5V (data not shown). VIVIT and INCA12 did not show any toxic effects in these cells. The above results clearly indicate that MCV1 is well tolerated by all major cell types relevant to the cardiovascular system and much less toxic than CsA.

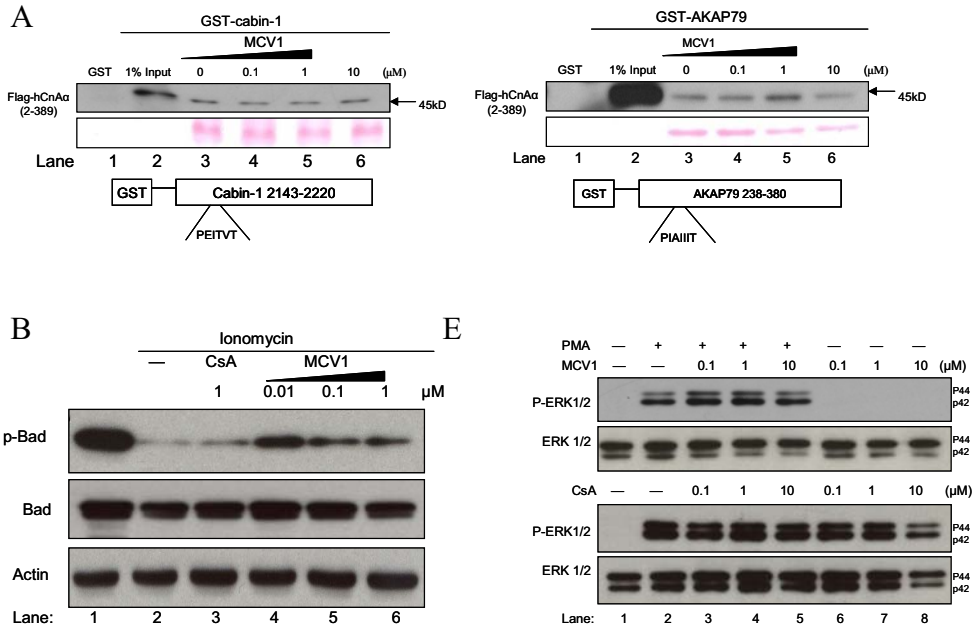

C

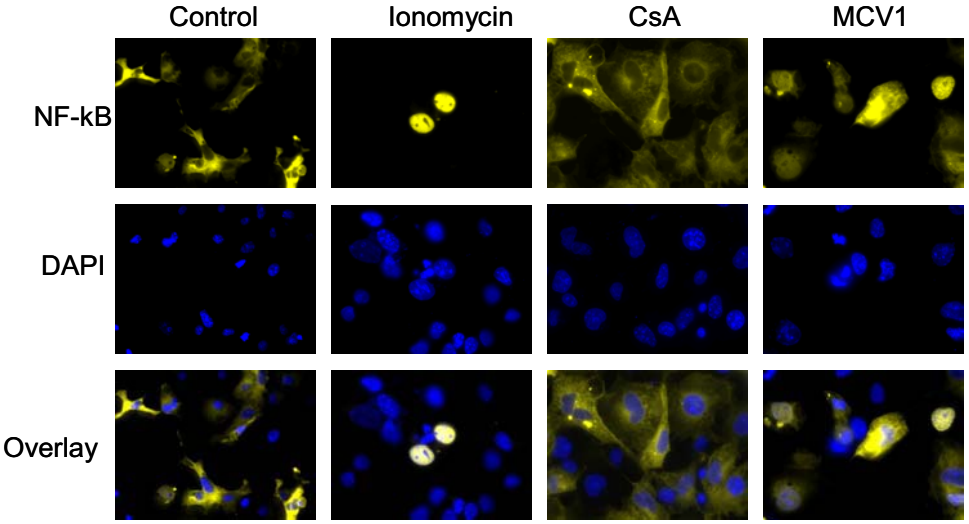
Control
Ionomycin
CsA
MCV1
NF-kB
DAPI
Overlay

D

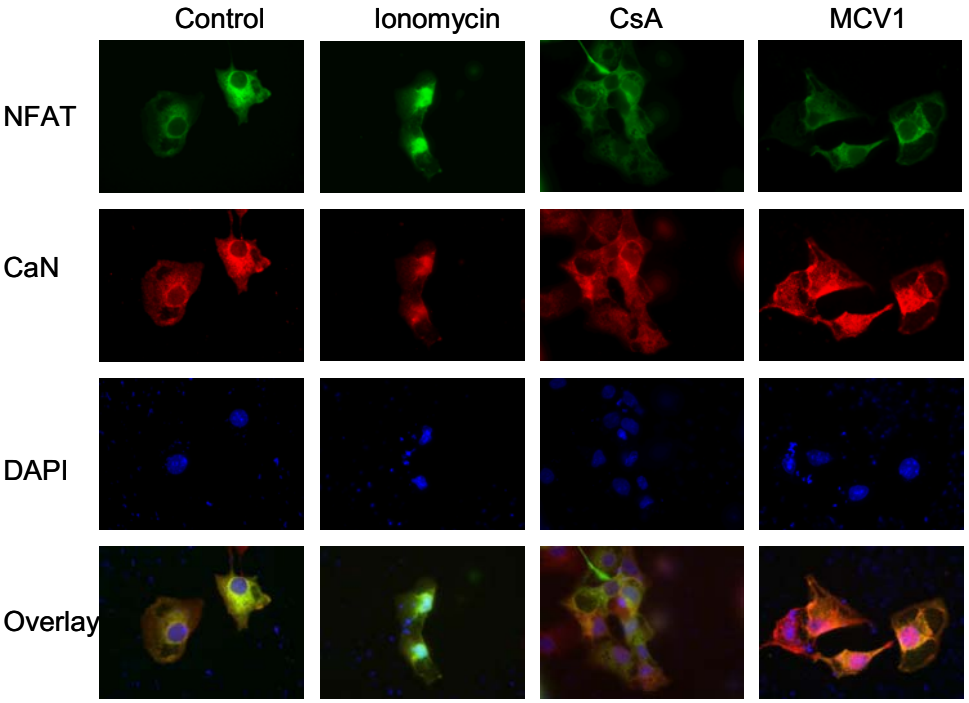
Control
Ionomycin
CsA
MCV1
NFAT
CaN
DAPI
Overlay

F

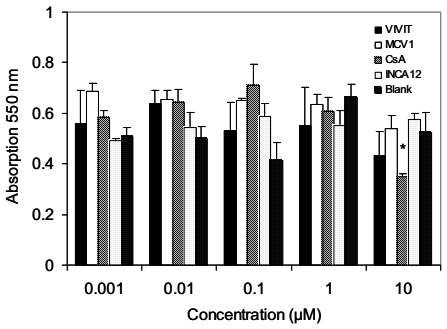

Figure 3: MCV1 is more selective for NFAT and less toxic than CsA. (A) Lysates from HEK-293 cells expressing FLAG-tagged CnA protein were analyzed by affinity binding to GST, GST-AKAP79 and GST-Cabin in the presence of MCV1 at the indicated concentrations. Bound protein was evaluated by Western blotting against FLAG tag. Ponceau S staining is provided to illustrate equal loading of the samples. **(B)** COS-1 cells transfected with pEBG-mBAD plasmid were incubated with 2 μM ionomycin for 24 hours in the presence of CsA or MCV1. Inhibition of Bad dephosphorylation was evaluated by Western blotting against phosphor-BAD (Ser136). Immunostaining against total Bad and anti-actin control are shown as a loading control. **(C)** YFP-p65 transfected COS-1 cells were stimulated for 20 min with ionomycin (1 μM) in the presence or absence of CsA (1μM**)** or MCV1 (1μM**).** Representative microscopic views illustrating that ionomycin elicited nuclear translocation of YFP-p65 (yellow) is prevented by CsA but not by MCV1. Nuclear staining with DAPI (blue) and overlay were also shown. **(D)** COS-1 cells were transfected with pNFAT1-GFP and 24 h later stimulated for 20 min with ionomycin (1 μM) in the presence or absence of CsA (1μM**)** or MCV1 (1μM**).** Cellular localization of calcineurin was visualized by anti-calcineurin and goat anti-rabbit conjugated Alexa Fluor 555 antibody staining. Nuclear DNA was labeled by DAPI (blue). NFAT1-GFP (green) co-localization with stained calcineurin (red) can be observed in the overlay (pink). **(E)** Growth-arrested vSMC were stimulated with or without 20 nM PMA, 1h after pretreatment for 15 min with MCV1 (upper) or CsA (lower) at the indicated concentrations. Cell lysates were subjected to protein immunoblotting and probed with anti-phospho-p42/p44 antibody. Total ERK antibody staining is shown as a loading control. **(F)** RAW 264.7 cells were incubated for 24h with VIVIT, MCV1, CsA and INCA12 at indicated concentrations. The toxic effect to the cell proliferation was measured in a MTT assay. Values represent means ±SD of three individual experiments (* $P<0.05$ versus control).

Discussion

Therapeutic agents with high affinity, good bioavailability, metabolic stability, and low toxicity are highly preferred in immunosuppressive drug discovery. The usage of CsA/FK506 is associated with toxicity and malignancy, which will disrupt all of calcineurin downstream effectors, including NFAT. Although VIVIT were found to be more selective than CsA, its low micromolar affinity would be the major setback demanded to improve for clinical application. In an attempt to facilitate the peptide entry into the cells, Noguchi et al conjugating VIVIT to the C-terminal of a cell-permeable peptide tag. The potency of VIVIT increased but to a limited extent[34]. As moderate affinity between calcineurin and NFAT may be preferred to prevent NFAT from activation in resting cells[35], it may be difficult to develop potent inhibitors based on the PxIxIT motif without affecting the calcineurin phosphatase activity. Moreover, VIVIT itself was identified by a combinatorial peptide repertoire suggesting that a further increase in VIVIT affinity solely by replacement of backbone peptide will be difficult to be obtained. We therefore sought to optimize the peptide by side group modification. By stepwise

optimization, we identified the minimal motif of VIVIT, HPVIVIT, required for effective inhibition of NFAT transcription and NFAT mediated vSMC proliferation. Subsequent side group modification led to successful design of the bipartite inhibitor MCV with low nanomolar potency (IC50=2 nM) for NFAT inhibition, representing a more than ten thousands fold increase as compared with VIVIT. In fact, it was equally potent as CsA. Previously we have successfully pursued a similar strategy to improve the affinity of a P-selectin peptide antagonist[36]. This strategy combined with combinatorial chemistry and side group modification of peptide inhibitors selected from natural library proves useful in the design of high-affinity ligands.

The surprisingly high affinity of MCV1 may result from three factors. Firstly, we envisioned to simultaneously target two separate NFAT docking sites of calcineurin arguing that linking of two weaker binders may accompany by a tremendous affinity gain[37]. For instance, a K_d=19 nM affinity compounds was generated by tethering two weak ligands (K_d=2 μM and 100 μM) of FK506 binding protein (FKBP)[38]. Theoretically the free energy of MCV1 binding to calcineurin will be the sum of the free energies of HPVIVIT and MPB plus a term. The dramatic gain in potency of MCV peptide seems to support this bipartite inhibitor theory. Secondly, the high affinity of MCV compounds may be attributable to a covalent interaction of their maleimido groups with Cys266 of calcineurin. Since INCA12 and HPVIVIT are relatively modest NFAT inhibitor, targeting to either of them is not sufficient to explain the affinity gain of MCV1. The docking energy for MCV1 was almost identical to that reported for PVIVIT binding to calcineurin, suggesting that there may have a different background. Conceivably, the binding mode showed in our study may reflect an initial step in MCV1 binding to calcineurin A (CnA). An allosteric change may be induced on the β11- β12 loop and the flipping away of this loop make the side chain of Cys266 more accessible by maleimido group of MCV1. Thirdly, VIVIT and HPVIVIT are highly hydrophilic. However, when coupled at the N-terminal end the INCA mimics such as 3-MBA or MPB, the MCV analogues exhibit rather lipophilic characteristic and are soluble in Dimethyl Sulfoxide (DMSO) but not H_2O. In this regard, the increased affinity of MCV1 is at least partly arisen from its lipophilic nature.

Considerable uncertainty remains regarding to the VIVIT peptide binding site on calcineurin. It was proposed that the core docking site of calcineurin on VIVIT motif comprises a proline pocket adjacent to the β13- β14 turn of calcineurin catalytic domain[39]. Our results from MCV1 docking model demonstrate that VIVIT is more likely to bind to β11- β12 turn of calcineurin A unit, which fits very well with the previous hypothesis that INCA compounds are capable of inducing an allosteric change of the VIVIT binding cleft at the β11- β12 loop of calcineurin[40]. While HPVIVIT and INCA12 both are weak inhibitors of calcineurin-NFAT interaction, simultaneous targeting of both NFAT recognition sites on calcineurin by MCV1 will result in the observed dramatic gain in affinity. Further refinement

of the maleimide group of MCV1 may pave the way to the development of even better inhibitors of NFAT activation.
MCV1 was seen to selectively interrupt the calcineurin interaction with NFAT leaving that of other calcineurin endogenous inhibitors, AKAP79 or Cabin-1 unaffected. Previous reports suggested that multiple sites of AKAP79 are responsible for calcineurin binding[41]. Also, NFAT likely binds to a different PxIxIT binding pocket than AKAP79[42] explaining why MCV1 does not displace AKAP79/Cabin-1 at concentrations disrupting NFAT/CaN association. In addition, MCV1 was found to be much more selective than CsA in that it does not influence the NF-κB signaling and CaN nuclear translocation. The co-translocation of calcineurin-NFAT was seen to be totally blocked by CsA but not MCV1. Therefore, MCV1 selectively prevents calcineurin-NFAT protein-protein association rather than acting on the calcineurin catalytic sites, which will translate into a greatly reduced toxicity. Furthermore, CsA boosted endogenous ERK phosphorylation at concentrations as low as 0.1 μM. Apart from interfereing with the calcineurin-NFAT axis CsA apprarently acts on other signaling targets, including ERK. Thus, CsA not only promotes dephosphorylation of NFAT but also facilitates its phosphorylation via activation of the ERK pathway. This dual action of CsA also explains why it is such a potent NFAT inhibitor in comparison to the VIVIT parent peptide, which only inhibits NFAT dephosphorylation. In general, MCV1 is more selective in dissection of NFAT signaling and less toxic than CsA under physiological conditions relevant to immuno- and cardiovascular therapy. While MCV1 displays a sustained activity *in vitro*, suggesting a reasonably high stability. A minor concern of MCV compounds will be the general reactivity of maleimido group to sulfhydryl groups and the peptide stability *in vivo*. These issues can be overcome by replacing the maleimido group with milder cysteine reactive constituents and generating D-peptide or peptidemimics, respectively.
In conclusion, we have designed a bipartite peptide inhibitor of NFAT with nanomolar potency, showing superior selectivity for NFAT and reduced toxicity over CsA. We expect that MCV leads not only represent new research tools for exploring calcineurin-NFAT signaling but also constitute excellent candidates in the generation of novel, selective anti-inflammatory and anti-proliferative drugs.

Acknowledgement
We are very grateful to Dr. A. Rao (Harvard Medical School) for providing the GFP-NFAT1 plasmid; and to Dr. MD Lopez and Dr. JM. Redondo (Madrid Heart Center) and Dr. Yanchao Huang (LUMC) for their kind help on pull-down assay; Dr. Chi-wing Chow (Albert Einstein College of Medicine) is acknowledged for the stimulating discussion and helpful comments.

Sources of Funding
This study was financially supported by grants LFA5952 from Technology Foundation STW. This study was also supported by grants 2003T.201 from the

Netherlands Heart Foundation. The authors belong to the European Vascular Genomics Network (http://www.evgn.org), a Network of Excellence supported by the European Community's Sixth Framework Program for Research Priority 1 (Life Sciences, Genomics, and Biotechnology for Health; contract LSHM-CT-2003-503254).

References

1. Aramburu,J., Rao,A. & Klee,C.B. Calcineurin: from structure to function. *Curr. Top. Cell Regul.* **36**, 237-295 (2000).
2. Rao,A., Luo,C. & Hogan,P.G. Transcription factors of the NFAT family: regulation and function. *Annu. Rev. Immunol.* **15**, 707-747 (1997).
3. Crabtree,G.R. Generic signals and specific outcomes: signaling through Ca2+, calcineurin, and NF-AT. *Cell* **96**, 611-614 (1999).
4. Molkentin,J.D. *et al.* A calcineurin-dependent transcriptional pathway for cardiac hypertrophy. *Cell* **93**, 215-228 (1998).
5. Izumo,S. & Aoki,H. Calcineurin--the missing link in cardiac hypertrophy. *Nat. Med.* **4**, 661-662 (1998).
6. Chin,E.R. *et al.* A calcineurin-dependent transcriptional pathway controls skeletal muscle fiber type. *Genes Dev.* **12**, 2499-2509 (1998).
7. Semsarian,C. *et al.* Skeletal muscle hypertrophy is mediated by a Ca2+-dependent calcineurin signalling pathway. *Nature* **400**, 576-581 (1999).
8. Musaro,A., McCullagh,K.J., Naya,F.J., Olson,E.N. & Rosenthal,N. IGF-1 induces skeletal myocyte hypertrophy through calcineurin in association with GATA-2 and NF-ATc1. *Nature* **400**, 581-585 (1999).
9. Griffith,J.P. *et al.* X-ray structure of calcineurin inhibited by the immunophilin-immunosuppressant FKBP12-FK506 complex. *Cell* **82**, 507-522 (1995).
10. Kissinger,C.R. *et al.* Crystal structures of human calcineurin and the human FKBP12-FK506-calcineurin complex. *Nature* **378**, 641-644 (1995).
11. Sigal,N.H. *et al.* Is cyclophilin involved in the immunosuppressive and nephrotoxic mechanism of action of cyclosporin A? *J. Exp. Med.* **173**, 619-628 (1991).
12. Hojo,M. *et al.* Cyclosporine induces cancer progression by a cell-autonomous mechanism. *Nature* **397**, 530-534 (1999).
13. Kiani,A., Rao,A. & Aramburu,J. Manipulating immune responses with immunosuppressive agents that target NFAT. *Immunity.* **12**, 359-372 (2000).
14. Aramburu,J. *et al.* Selective inhibition of NFAT activation by a peptide spanning the calcineurin targeting site of NFAT. *Mol. Cell* **1**, 627-637 (1998).
15. Aramburu,J. *et al.* Affinity-driven peptide selection of an NFAT inhibitor more selective than cyclosporin A. *Science* **285**, 2129-2133 (1999).
16. Roehrl,M.H. *et al.* Selective inhibition of calcineurin-NFAT signaling by blocking protein-protein interaction with small organic molecules. *Proc. Natl. Acad. Sci. U. S. A* **101**, 7554-7559 (2004).
17. Kang,S., Li,H., Rao,A. & Hogan,P.G. Inhibition of the calcineurin-NFAT interaction by small organic molecules reflects binding at an allosteric site. *J. Biol. Chem.* **280**, 37698-37706 (2005).

18. Roehrl,M.H. *et al.* Selective inhibition of calcineurin-NFAT signaling by blocking protein-protein interaction with small organic molecules. *Proc. Natl. Acad. Sci. U. S. A* **101**, 7554-7559 (2004).
19. Kang,S., Li,H., Rao,A. & Hogan,P.G. Inhibition of the calcineurin-NFAT interaction by small organic molecules reflects binding at an allosteric site. *J. Biol. Chem.* **280**, 37698-37706 (2005).
20. Yu,H. *et al.* Therapeutic potential of a synthetic peptide inhibitor of nuclear factor of activated T cells as antirestenotic agent. *Arterioscler. Thromb. Vasc. Biol.* **26**, 1531-1537 (2006).
21. Rodriguez,A., Martinez-Martinez,S., Lopez-Maderuelo,M.D., Ortega-Perez,I. & Redondo,J.M. The linker region joining the catalytic and the regulatory domains of CnA is essential for binding to NFAT. *J. Biol. Chem.* **280**, 9980-9984 (2005).
22. Li,H., Rao,A. & Hogan,P.G. Structural delineation of the calcineurin-NFAT interaction and its parallels to PP1 targeting interactions. *J. Mol. Biol.* **342**, 1659-1674 (2004).
23. Aramburu,J. *et al.* Selective inhibition of NFAT activation by a peptide spanning the calcineurin targeting site of NFAT. *Mol. Cell* **1**, 627-637 (1998).
24. Aramburu,J. *et al.* Affinity-driven peptide selection of an NFAT inhibitor more selective than cyclosporin A. *Science* **285**, 2129-2133 (1999).
25. Yu,H. *et al.* Therapeutic potential of a synthetic peptide inhibitor of nuclear factor of activated T cells as antirestenotic agent. *Arterioscler. Thromb. Vasc. Biol.* **26**, 1531-1537 (2006).
26. Kang,S., Li,H., Rao,A. & Hogan,P.G. Inhibition of the calcineurin-NFAT interaction by small organic molecules reflects binding at an allosteric site. *J. Biol. Chem.* **280**, 37698-37706 (2005).
27. Li,H., Rao,A. & Hogan,P.G. Structural delineation of the calcineurin-NFAT interaction and its parallels to PP1 targeting interactions. *J. Mol. Biol.* **342**, 1659-1674 (2004).
28. Liu,J.O. Endogenous protein inhibitors of calcineurin. *Biochem. Biophys. Res. Commun.* **311**, 1103-1109 (2003).
29. Dell'Acqua,M.L., Dodge,K.L., Tavalin,S.J. & Scott,J.D. Mapping the protein phosphatase-2B anchoring site on AKAP79. Binding and inhibition of phosphatase activity are mediated by residues 315-360. *J. Biol. Chem.* **277**, 48796-48802 (2002).
30. Wang,H.G. *et al.* Ca2+-induced apoptosis through calcineurin dephosphorylation of BAD. *Science* **284**, 339-343 (1999).
31. Wang,H.G. *et al.* Ca2+-induced apoptosis through calcineurin dephosphorylation of BAD. *Science* **284**, 339-343 (1999).
32. Timmerman,L.A., Clipstone,N.A., Ho,S.N., Northrop,J.P. & Crabtree,G.R. Rapid shuttling of NF-AT in discrimination of Ca2+ signals and immunosuppression. *Nature* **383**, 837-840 (1996).
33. Shibasaki,F., Price,E.R., Milan,D. & McKeon,F. Role of kinases and the phosphatase calcineurin in the nuclear shuttling of transcription factor NF-AT4. *Nature* **382**, 370-373 (1996).
34. Noguchi,H. *et al.* A new cell-permeable peptide allows successful allogeneic islet transplantation in mice. *Nat. Med.* **10**, 305-309 (2004).
35. Aramburu,J. *et al.* Affinity-driven peptide selection of an NFAT inhibitor more selective than cyclosporin A. *Science* **285**, 2129-2133 (1999).

36. Appeldoorn,C.C. *et al.* Rational optimization of a short human P-selectin-binding peptide leads to nanomolar affinity antagonists. *J. Biol. Chem.* **278**, 10201-10207 (2003).
37. Hajduk,P.J., Meadows,R.P. & Fesik,S.W. Discovering high-affinity ligands for proteins. *Science* **278**, 497,499 (1997).
38. Shuker,S.B., Hajduk,P.J., Meadows,R.P. & Fesik,S.W. Discovering high-affinity ligands for proteins: SAR by NMR. *Science* **274**, 1531-1534 (1996).
39. Li,H., Rao,A. & Hogan,P.G. Structural delineation of the calcineurin-NFAT interaction and its parallels to PP1 targeting interactions. *J. Mol. Biol.* **342**, 1659-1674 (2004).
40. Kang,S., Li,H., Rao,A. & Hogan,P.G. Inhibition of the calcineurin-NFAT interaction by small organic molecules reflects binding at an allosteric site. *J. Biol. Chem.* **280**, 37698-37706 (2005).
41. Dell'Acqua,M.L., Dodge,K.L., Tavalin,S.J. & Scott,J.D. Mapping the protein phosphatase-2B anchoring site on AKAP79. Binding and inhibition of phosphatase activity are mediated by residues 315-360. *J. Biol. Chem.* **277**, 48796-48802 (2002).
42. Kashishian,A. *et al.* AKAP79 inhibits calcineurin through a site distinct from the immunophilin-binding region. *J. Biol. Chem.* **273**, 27412-27419 (1998).